A Simple Technique for Islanding Detection With Negligible Nondetection Zone

H. H. Zeineldin, *Member, IEEE*, and James L. Kirtley, Jr., *Fellow, IEEE*

Abstract—Although active islanding detection techniques have smaller nondetection zones than passive techniques, active methods could degrade the system power quality and are not as simple and easy to implement as passive methods. The islanding detection strategy, proposed in this paper, combines the advantages of both active and passive islanding detection methods. The distributed-generation (DG) interface was designed so that the DG maintains stable operation while being grid connected and loses its stability once islanded. Thus, the over/undervoltage and over/underfrequency protection method would be sufficient to detect islanding. The main advantage of the proposed technique is that it relies on a simple approach for islanding detection and has negligible nondetection zone. The system was simulated on PSCAD/EMTDC and simulation results are presented to highlight the effectiveness of the proposed technique.

Index Terms—Distributed generation (DG), inverter, islanding, over/underfrequency, over/under voltage.

I. INTRODUCTION

ISLANDING is a condition in which a part of the utility system, which contains load and generation, is isolated from the rest of the utility system and continues to operate. An islanding event could occur as a result of a fault on the upstream feeder of a distribution substation which could lead to the operation of the main feeder recloser. The recloser will attempt to close after a certain time interval (usually between 500 ms to 1 s). The islanding detection method should be capable of operating in a timely manner to avoid damages that could result from reclosing on an energized network.

There are three main categories for islanding detection methods which include: 1) passive, 2) active, and 3) communication-based methods. Passive methods rely on monitoring a certain parameter and then setting thresholds on the selected parameter. Despite its simplicity and easiness to implement, passive methods suffer from large nondetection zones (NDZs). NDZs could be defined as the loading conditions for which an islanding detection method would fail to operate in a timely manner. Selecting suitable thresholds for passive methods that rely on monitoring THD and voltage unbalance becomes a hard and complex task since these parameters are system

dependent [1]. Active methods introduce deliberate changes or disturbances to the connected circuit and then monitor the response to determine an islanding condition [2]. Active methods have smaller NDZ but, on the other hand, can degrade the power quality of the system [2]. In addition, some active methods require the implementation of addition controllers which increases the complexity of the islanding detection method [3]–[5]. Communication-based methods have negligible NDZ but are more expensive than the former methods. A comprehensive survey on the different islanding detection methods could be found in [2] and [6].

In this paper, we aim to develop a new islanding detection technique that would incorporate the advantages of the three islanding detection categories while avoiding their drawbacks. The DG interface control under study is designed to operate at unity power factor and the load is modeled as a constant RLC load. The proposed method relies on designing the DG interface so that the DG maintains stable operation while being grid connected and loses its stability once islanded. A simple and easy to implement method, such as the over/undervoltage and over/underfrequency protection (OVP/UVP and OFP/UFP), is used to detect an islanding condition. The OVP/UVP and OFP/UFP method relies on monitoring the voltage and frequency at the DG interconnection point. Once the magnitude of either one exceeds a prespecified threshold value, an islanding condition is declared and the DG is disconnected.

The paper is organized as follows: Section II presents the system and DG interface model under study. Section III presents the proposed islanding detection method. Section IV provides simulation results that highlight the performance of the proposed islanding detection technique. Section V highlights the impacts of system voltage variations on the proposed technique and presents an extension to the proposed islanding detection method. Finally, conclusions are drawn in Section VI.

II. SYSTEM UNDER STUDY

The system, shown in Fig. 1, consists of a distribution network represented by a source behind impedance, a load represented in terms of R-L-C, and a 100 kW inverter-based DG. The DG interface control model presented in [7] was implemented. The DG is designed to operate as a constant power source by setting the controller's active and reactive reference values to fixed values. The reactive power reference value (Q_{ref}) is set to zero, thus simulating a unity power factor DG operation. The DG interface has two sets of controllers: 1) for power regulation and 2) for current regulation as shown in Fig. 2. The load is represented as a constant RLC load with an active and reactive

H. H. Zeineldin is with the Masdar Institute of Science and Technology, Abu Dhabi, United Arab Emirates (e-mail: hatem@MIT.EDU).

J. L. Kirtley, Jr. is with the Massachusetts Institute of Technology, Cambridge, MA 02139 USA.
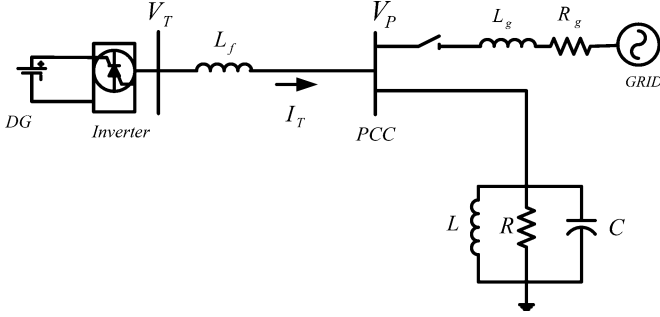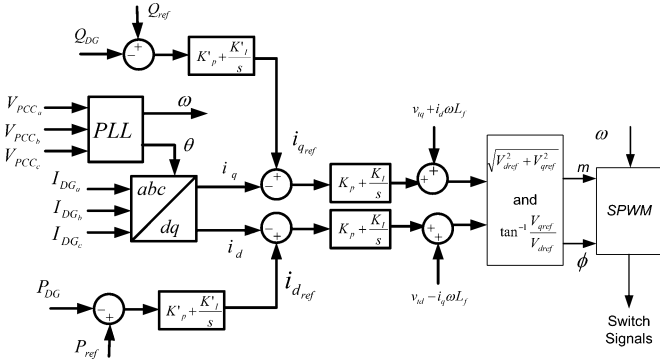
Fig. 1. System under study.

Fig. 2. DG interface control for constant power operation.

power expressed as shown in (1) and (2)

$$P = P_o \left(\frac{V}{V_o} \right)^2 \qquad (1)$$

$$Q = Q_o \left(\frac{V}{V_o} \right)^2 \qquad (2)$$

where V_o represents the initial operating voltage and P_o and Q_o represent the active and reactive power corresponding to the initial operating voltage. The inductive and capacitive components of the load are modeled by using (2).

The DG interface control variables are controlled by using the d–q synchronous reference frame. The instantaneous real and reactive power could be written in terms of the d–q axis components as follows [5], [8]:

$$P = \frac{3}{2} v_{pd} i_{td} \qquad (3)$$

$$Q = \frac{3}{2} v_{pd} i_{tq} \qquad (4)$$

where v_{pd} is the d-axis component of the PCC voltage and is equivalent to the phase peak value at the PCC. The parameters i_{td} and i_{tq} are the d–q components of the DG currents. Under balanced conditions, the d–q components of the voltage and current are constant quantities. The two current components are decoupled which facilitates independent regulation of the real and reactive power. The instantaneous voltages of the three phases could be expressed as follows [5], [8]:

$$\frac{d}{dt} i_{tabc} = -\frac{R_f}{L_f} i_{tabc} + \frac{1}{L_f} (v_{tabc} - v_{pabc}) \qquad (5)$$
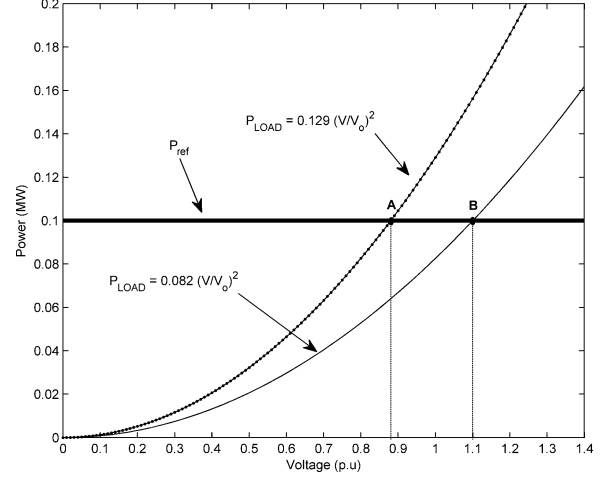
Fig. 3. Power versus voltage characteristic for the DG and load with P_{ref} set to 100 kW.

where i_{tabc} represents the DG current three-phase components. R_f and L_f represent the filter resistance and inductance. Variables v_{tabc}, and v_{pabc} represent the DG terminal and PCC three-phase voltages. By using Park's transformation [8], (5) can be transformed to the synchronously rotating reference frame as follows [5], [8]:

$$\frac{d}{dt} \begin{bmatrix} i_{td} \\ i_{tq} \end{bmatrix} = \begin{bmatrix} -\frac{R_f}{L_f} & \omega \\ -\omega & -\frac{R_f}{L_f} \end{bmatrix} \begin{bmatrix} i_{td} \\ i_{tq} \end{bmatrix} + \frac{1}{L_f} \begin{bmatrix} v_{td} - v_{pd} \\ v_{tq} - v_{pq} \end{bmatrix}. \qquad (6)$$

The DG interface control is developed by using the set of equations as shown in Fig. 2. The magnitude and angle of the modulating signal are calculated and are used to determine the inverter switching signal.

III. PROPOSED ISLANDING DETECTION TECHNIQUE

The IEEE Std. 1547 and UL 1741 provide thresholds on the amount of acceptable voltage and frequency deviation. Thresholds on voltage deviations are in the range of 88% to 110% of the nominal voltage value [9], [10]. Any voltage deviation, resulting from an islanding condition, within these limits, would not be detected and the corresponding load would be considered within the NDZ. The load and DG P–V characteristic are analyzed to determine the amount of voltage deviation. Since the DG is designed to operate at a constant active power output, the DG power curve is represented as a horizontal line at 100 kW. For constant RLC loads, the active power is proportional to the square of the voltage.

Fig. 3 illustrates the P–V characteristic of the DG and load. The point at which the DG and load curve intersect is called the islanding operating point. It can be seen that for an islanded load of 129 kW, the operating point "A" corresponds approximately to a voltage of 0.88 p.u. On the other hand, an 82-kW load corresponds approximately to a voltage of 1.1 p.u. The two loads represent the upper and lower active power limits. Any load with an active power curve between the two load curves presented in Fig. 3 is considered within the NDZ. The results coincide with the active power mismatch equation presented in [11].

It could be seen that one of the factors that results in the presence of an NDZ is the constant DG power curve. The active
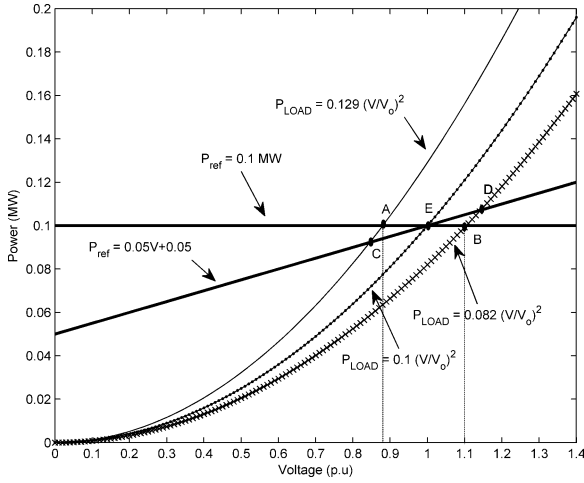
Fig. 4. Power versus voltage characteristic for the DG and load with P_{ref} expressed as a function of the voltage with a positive slope.

Fig. 5. Power versus voltage characteristic for the DG and load with P_{ref} expressed as a function of the voltage with a negative slope.

power mismatch of the NDZ is dependent on the DG P_{ref} setting. The DG reference power curve was modified and expressed as a function of its terminal voltage. The expression was formulated so that the DG delivers rated power at rated voltage. Fig. 4 presents the power versus voltage curves for three loading conditions and the DG. The DG reference power is expressed in terms of voltage as follows:

$$P_{\text{ref}} = 0.05V + 0.05. \tag{7}$$

The 100-kW load intersects the DG power curve at point "E" which corresponds to an active power of 100 kW and a voltage of 1 p.u. The 82-kW and 129-kW loads intersect the new DG curve at points "C" and "D". These two points correspond to voltage levels that are beyond the allowable voltage levels. Thus, these loading conditions will be easily detected using the over/ under voltage protection (OVP/UVP) method. The same two loading conditions were within the NDZ (points "A" and "B" in Fig. 3) when the DG reference power curve was set to be fixed at 100 kW. Thus, a reduction in the NDZ could be achieved by expressing P_{ref} as a function of voltage. This is the main idea behind the proposed technique.

Even though the NDZ has been reduced, we further explore different power-voltage expressions to identify the mathematical expression that would result in the smallest NDZ. The reference power was further expressed as a function of voltage but with a negative slope and the expression is

$$P_{\text{ref}} = -0.06V + 0.16. \tag{8}$$

Fig. 5 presents the power versus voltage curves for three loading conditions and the DG. Similarly, the 100-kW load intersects the DG power curve at point "M" which corresponds to an active power of 100 kW and a voltage of 1 p.u. The 82-kW and 129-kW loads intersect the new DG curve at points C' and D'. These two points correspond to voltage levels that are within the allowable voltage levels. Thus, these loading conditions will not be detected by using the OVP/UVP method and are within the NDZ. The same two loading conditions were
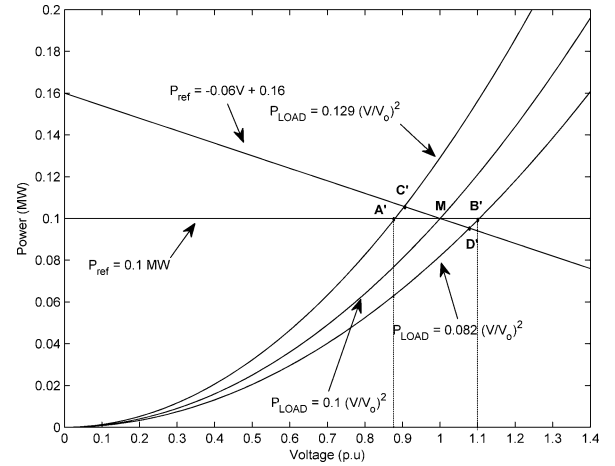
at the border of the NDZ (points "A" and "B") when the DG reference power curve was set to be fixed at 100 kW. Thus, using a power-voltage expression with a negative slope will lead to an increase in the NDZ.

By comparing Figs. 4 and 5, it can be seen that a P–V expression with a positive slope can reduce the NDZ of the OVP/UVP method. To further reduce the NDZ, the slope of the DG curve is increased until it reaches a point where the DG curve becomes a tangent to the 100 kW load curve. The DG P_{ref} could be expressed as follows:

$$P_{\text{ref}} = 0.2V - 0.1 \tag{9}$$

Fig. 6 presents the power versus voltage curves for three loading conditions and the DG curve presented in (9). As shown in Fig. 6, the 100 kW load intersects the DG power curve at point "C" which corresponds to an active power of 100 kW and a voltage of 1 p.u. For loads that are greater than 100 kW, the DG P_{ref} curve will not intersect the load curves and, thus, the DG will become unstable for loads greater than 100 kW. For the 82 kW load, the DG P_{ref} curve will intersect at point "D" (refer to Fig. 6) and another point that is outside the graph window. For a small perturbation to the right of point "D," DG power generation would be greater than the load and this would result in an increase in the operating voltage. Thus, point "D" is an unstable islanding operating point.

Based on the aforementioned analysis, the proposed islanding detection technique in this section relies on the following:
1) setting the DG P_{ref} to be a function of the voltage;
2) setting the DG P_{ref} to be a tangent to (1) at rated conditions. The general formula for calculating P_{ref} could be represented as follows:

$$\frac{P_{\text{ref}} - P_o}{V - V_o} = \left. \frac{dP}{dV} \right|_{P_o, V_o} \tag{10}$$

$$P_{\text{ref}} = P_o + 2P_o(V - V_o) \tag{11}$$

where P_o represents the DG rated active power capacity in MW (set to 0.1 MW for the case presented) and V_o represents the rated voltage in per unit (set to 1 p.u.). The proposed formula
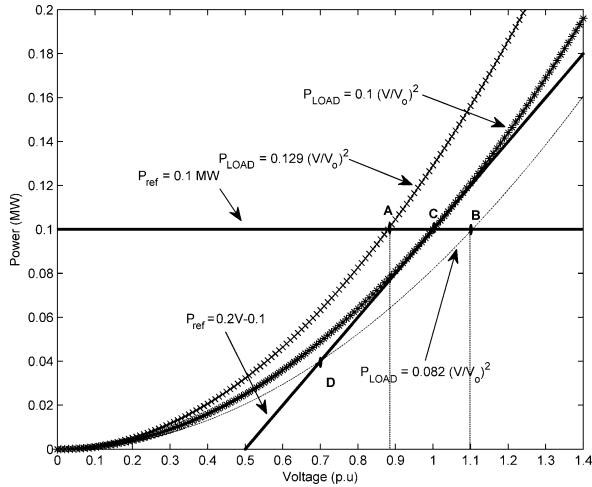
Fig. 6. Power versus voltage characteristic for the DG and load with P_{ref} expressed as a function of the voltage and tangent to the 100 kW load curve.
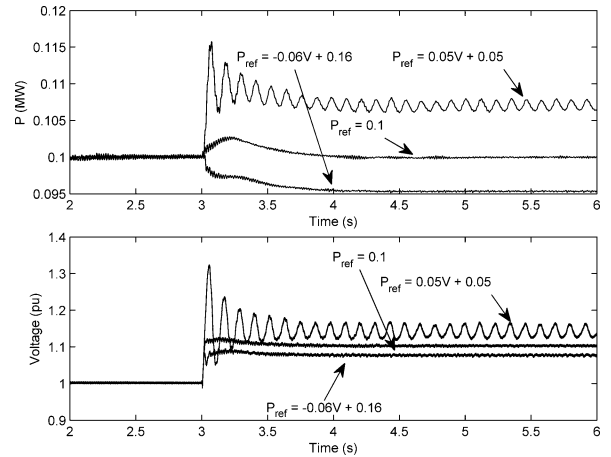

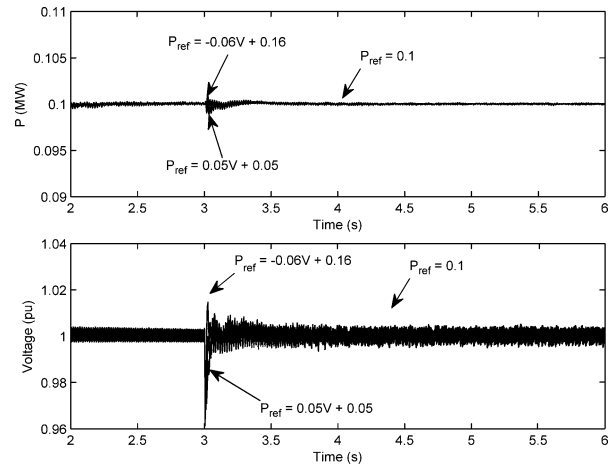Fig. 7. Active power and voltage for the 82 kW loading condition.

Fig. 8. Active power and voltage for the 100 kW loading condition.

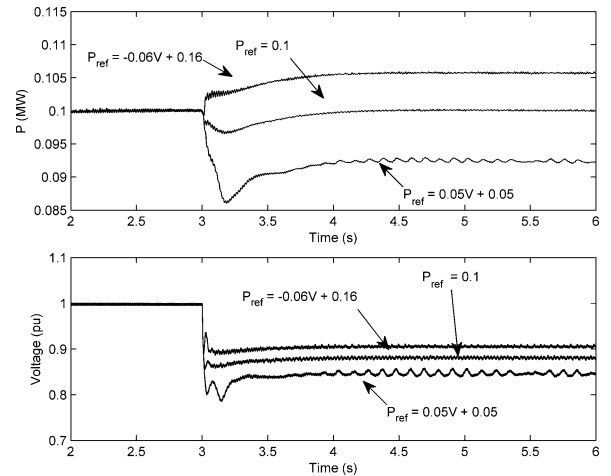Fig. 9. Active power and voltage for the 129 kW loading condition.

could be easily integrated in the DG interface control by monitoring and calculating the point of common coupling (PCC) per unit voltage and then performing the mathematical operations dictated by (11).

The technique does not require any additional control blocks. A simple and easy-to-implement islanding protection method, such as the OVP/UVP method, is implemented to detect the deviation in voltage once an islanding condition occurs. The analysis shows that by using the proposed P–V expression, the OVP/UVP will have negligible NDZ.

IV. Performance of the Proposed Islanding Detection Technique During an Islanding Condition

The proposed islanding detection method was tested on the system shown in Fig. 1. An islanding condition is simulated by opening the utility breaker at t $= 3$ s. First, the results presented in Section III are verified by setting the DG P_{ref} as expressed in (7) and (8) and monitoring the voltage for the three loading levels presented in Section III (129 kW, 100 kW, and 82 kW). Figs. 7– 9 show the active power and voltage waveforms obtained by using the time-domain simulations in the PSCAD/EMTDC environment for the various case studies.

For the 82 kW load, with P_{ref} set fixed at 100 kW, the voltage stabilizes at approximately a value of 1.1 p.u. and the load's active power adjusts itself to 100 kW. This is the common output expected for a DG operating with a fixed P_{ref} value [12]. For the case where P_{ref} increases with the increase in voltage (positive slope case), the voltage and power will settle at a value greater than 1.1 p.u. and 100 kW, respectively. This corresponds to point "D" which was presented in Fig. 4. For the case where P_{ref} decreases with the increase in voltage (negative slope case), the voltage and active power will be less than 1.1 p.u. and 100 kW, respectively. This corresponds to point D', which was presented in Fig. 5. It can be seen that for a DG with a positive P–V slope, the NDZ of the OVP/UVP method could be decreased. On the other hand, a negative P–V slope increases the NDZ.

For the 100 kW load, the voltage and power stabilize at a value of 1 p.u. and 100 kW for the three DG P–V curves. This corresponds to point "E" in Fig. 4 and "M" in Fig. 5. The

OVP/UVP method would fail to detect islanding for the three different scenarios. On the other hand, for the 129 kW case, the voltage will settle at a voltage of 0.88 p.u. with P_{ref} set fixed to 100 kW. This is the common output expected for a DG operating with a fixed P_{ref} value [12]. For the case where P_{ref} increases with the increase in voltage (positive slope case), the voltage
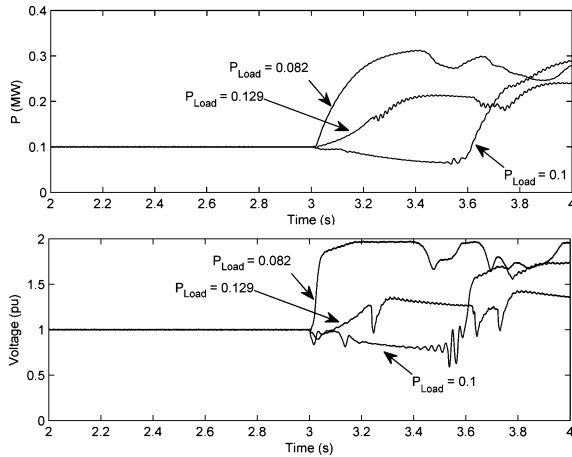
Fig. 10. Active power and voltage for $P_{\mathrm{ref}} = 0.2\,\mathrm{V} - 0.1$.

Fig. 11. PCC voltage and frequency for various different load quality factors (Q_f).

Fig. 12. PCC voltage with $P_{\mathrm{ref}} = 0.2\,\mathrm{V} - 0.1$ with two DGs in an islanded condition.

and power will settle at a value that is less than 0.88 p.u. and 100 kW, respectively. This corresponds to point "C" which was presented in Fig. 4. For the case where P_{ref} decreases with the increase in voltage (negative slope case), the voltage and active power will settle at a value greater than 0.88 p.u. and 100 kW, respectively. This corresponds to point C', which was presented in Fig. 5. Similarly, it can be concluded that with a positive P–V slope, the NDZ of the OVP/UVP method could be decreased.

The same case studies were examined but for the case where P_{ref} is set as expressed in (9). Fig. 10 presents the active power and the PCC voltage for three loading conditions. For the three loading conditions, the PCC voltage becomes unstable and islanding could be detected easily by using the OVP/UVP method. The results show that for very small mismatches in active power (100 kW case), the DG becomes unstable. With such a design, monitoring the PCC voltage would be a sufficient measure for detecting an islanding condition.

The UL 1741 standards specifies that an islanding condition should be detected within two seconds for RLC loads with a quality factor $(Q_f = R\sqrt{C/L})$ that is less than 1.8 [5], [10]. RLC loads with high values of Q_f are problematic for islanding detection [2]. Fig. 11 shows the PCC voltage and frequency for three different values of load quality factor. It can be seen that for the presented cases, the proposed islanding detection technique is capable of meeting the testing requirements. The islanding detection technique will be capable of detecting islanding in less than 200 ms.

Further, a multiple DG case was explored to investigate the effectiveness of the proposed islanding detection technique to islands with more than one DG. An additional 100-kW DG was added in parallel with the original one. The total island load was adjusted to 200 kW to match the two available DG capacities. The P_{ref} setting of both DGs was set as expressed in (9). Fig. 12 presents the PCC voltage with an islanding condition at t = 3 s. Similarly, it can be seen that once islanding occurs, the PCC voltage becomes unstable and the OVP/UVP method can easily detect an islanding condition. For the case study presented, the simulation results potentially show that the proposed islanding detection technique does not degrade with multiple DG on the island.
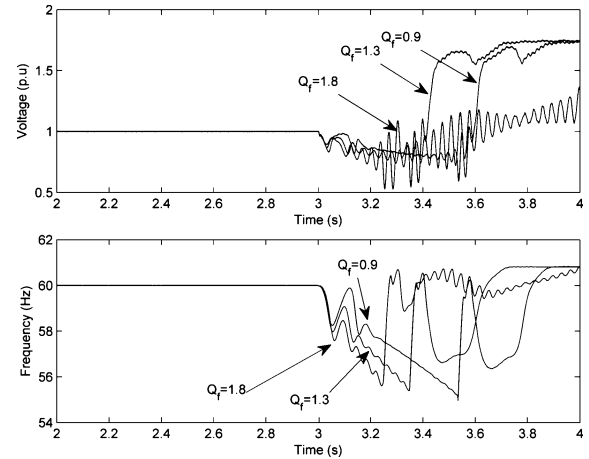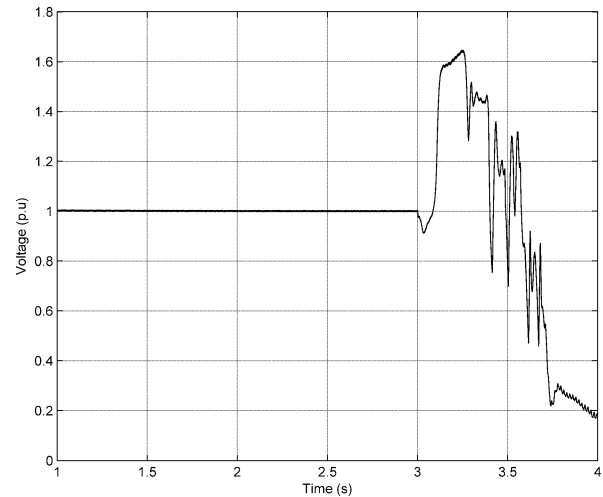
V. IMPACT OF VOLTAGE VARIATIONS ON THE PROPOSED ISLANDING DETECTION TECHNIQUE

Voltage variations on a distribution system could be classified into three main types based on the magnitude and duration of the voltage deviation. These three types include: 1) transient, 2) short-term voltage variation, and 3) long-term voltage variations. The duration of transient voltage variations are in the range of milliseconds. Short-term voltage variations, which include voltage sags and swells, can last up to 1 min. On the other hand, long-term voltage variations are voltage deviations that occur and last for more than 1 min [13]. These variations in voltage could be within the OVP/UVP thresholds while the DG is grid connected and it is expected that the DG would continue to operate efficiently during such deviations. For example, in [14], it was found that some spots on a rural distribution system operated at voltage levels that were either higher or lower than the nominal voltage but within the OVP/UVP levels. The voltage levels on 69 rural sites were examined and it was found that 25% of the sites experienced average long-term utilization voltage levels that were less than the nominal voltage while 75% experienced higher voltage levels [14].

The proposed islanding detection method, presented in Section III, relies on equipping the DG with a fixed P–V characteristic given in (9). For a system that experiences long-term voltage deviations that are between 88% and 110% of the nominal voltage level, occurring while the DG is grid connected, the DG output power would vary between 76 and 120 kW. This indicates that the DG would be overloaded and supply more than its rated output power (100 kW). In order to avoid such undesirable operating conditions, the DG P–V curve was adaptively shifted to the left or right based on the measured voltage. The P–V characteristic expressed in (11) could be rewritten as follows:

$$P_{\text{ref}} = aV_{\text{p.u.}} + b \tag{12}$$

where $a = 2P_o$ and $b = P_o - 2P_oV_o$ represent the P–V characteristic parameters. Instead of setting "b" in (12) to a fixed value, it would adaptively change based on the measured PCC voltage (V_m) as follows:

$$b = P_o - aV_m. \tag{13}$$

In order to maintain negligible NDZ, the DG P–V curve slope was chosen to be larger than the highest expected load slope within the OVP/UVP thresholds. In other words, the slope "a" can be written as follows:

$$a \geq \frac{dP}{dV} \tag{14}$$

$$a \geq 2P_o\frac{V}{V_o}. \tag{15}$$

The load that is within the NDZ of the OVP/UVP method with the highest slope corresponds to a load of 0.129 MW and an operating voltage of 1.1 p.u. For negligible NDZ, the slope of the P–V curve should be set to be larger than 0.2838 and was chosen to be equal to 0.3. Fig. 13 shows how varying "b" can shift the P–V curve to the left or right to maintain the active power at 1 p.u. during voltage variations. It can also be seen that points A, B, C, D, and E (refer to Fig. 13) are all unstable operating points and, thus, the method will maintain negligible NDZ.

The islanding detection technique, presented in Section III, was augmented with an active power comparator and a delayed pulse generator. The active power comparator is used to detect the instant at which a disturbance occurs. A time delay of 500 ms was introduced to allow sufficient time for the islanding detection method to operate in case of an islanding condition. During that period of time, b is kept fixed. For active power deviations that persist for more than 500 ms, the parameter b is switched from a fixed value to a variable value that relies on the measured voltage [refer to (13)]. The parameter b will be updated according to (13) until the active power is within the threshold limits. Once the active power is within limits, b will be fixed at its latest calculated value. Fig. 14 shows a flowchart of the P–V curve shifting procedure.

The extended islanding detection technique was implemented on PSCAD/EMTDC to examine the effect of long-term voltage variations. A voltage drop was initiated at t = 3 s and islanding was initiated at t = 5 s. Fig. 15 presents the DG active power

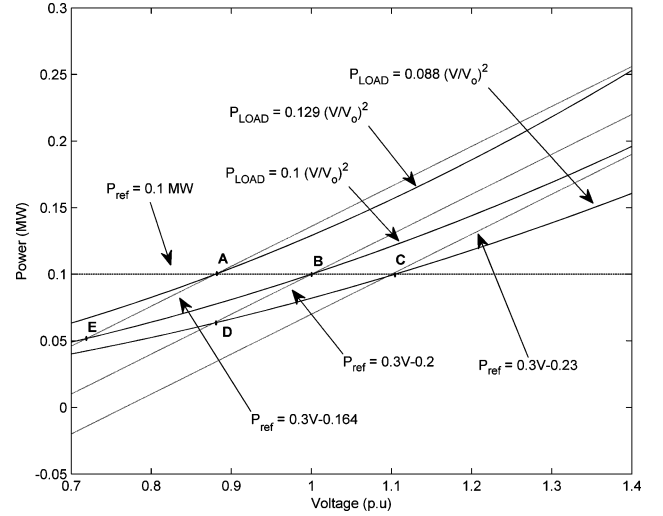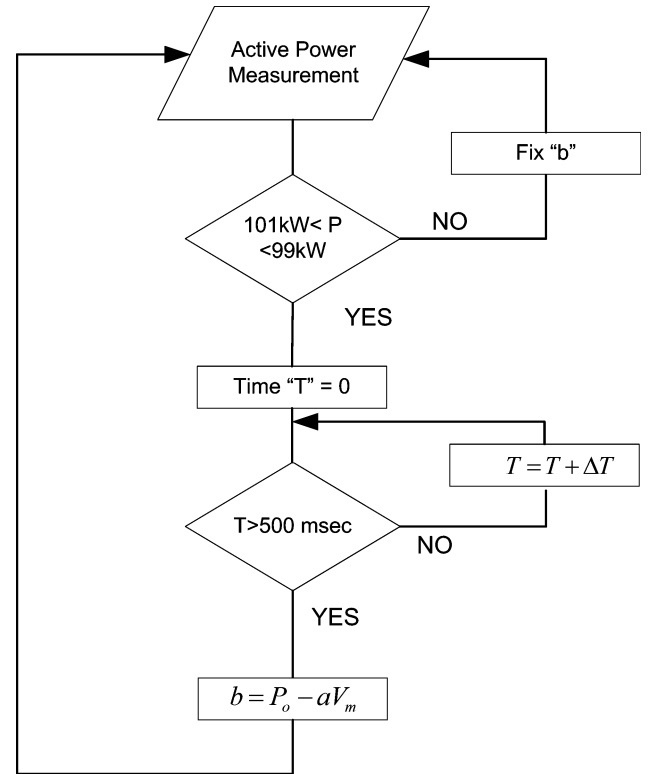Fig. 13.   Load curves and DG P–V characteristics for various values of b.

Fig. 14.   Flowchart showing the procedure for shifting the P–V curve.

output as well as the PCC voltage. It can be seen that the moment the voltage drops to approximately 0.9 p.u., the DG active power will drop to approximately 70 kW as a result of the DG P–V characteristic operation. The drop in active power remains for 500 ms and at t = 3.5 s, "b" is adaptively adjusted to adjust the active power output to 100 kW. It can be seen that by setting the DG P–V slope to be higher than the slope of the load curve, an islanding condition could be easily detected.

To conclude, for distribution systems with utilization voltages that are maintained close to and less than 1 p.u., the islanding detection method described in Section III would be sufficient. For other distribution systems with diverse utilization voltages that
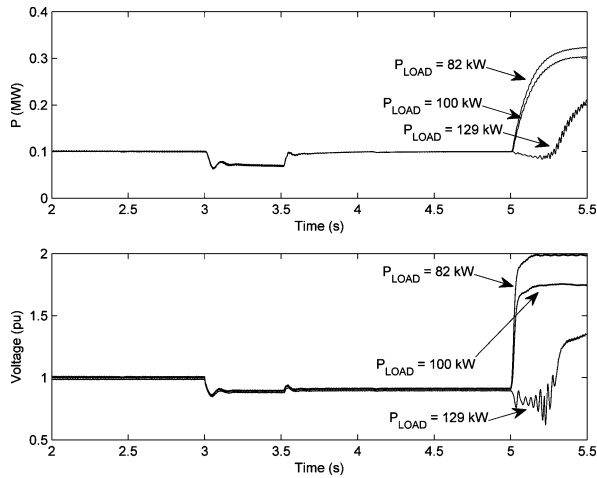
Fig. 15. DG active power output and PCC voltage during a voltage sag and an islanding event.

TABLE I
NDZ UPPER AND LOWER LIMITS FOR DIFFERENT P–V CHARACTERISTICS

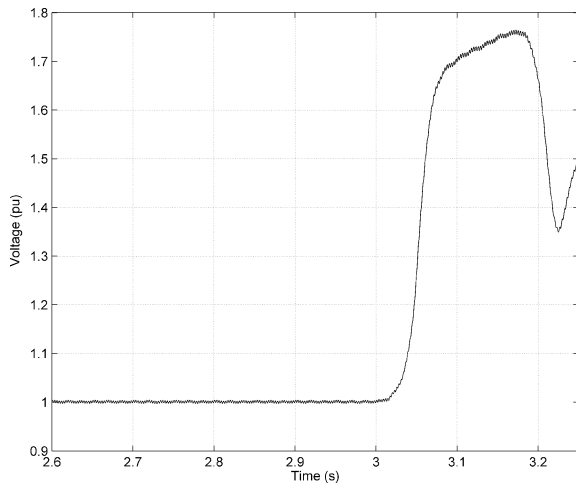|	a	b	NDZ Lower Limit (MW)	NDZ Upper Limit (MW)
Case 1	0	0.1	0.0826	0.129
Case 2	0.05	0.05	0.0868	0.1214
Case 3	-0.06	0.16	0.0777	0.1384
Case 4	0.2	-0.1	0.0981 (Unstable)	0.0992

Fig. 16. PCC voltage with $P_{\text{ref}} = 0.2 V - 0.1$ with an islanded load of 99 kW.

vary between 88% to 110% of the nominal voltage, the extended proposed technique presented in this section would be necessary to ensure negligible NDZ and efficient DG operation.

VI. CONCLUSION

This paper presents a new simple and easy-to-implement approach for islanding detection. The proposed idea relies on examining the P–V characteristic of the DG and load, and determining the best operating characteristic for the DG that will aid in islanding detection. The P–V characteristic of the DG was chosen so that the DG maintains stable operation while it

is grid connected and loses its stability once islanded. The PCC voltage is monitored and the OVP/UVP method is used to disconnect the DG once it is islanded. The main advantages of the proposed technique include:

1) unlike some of the previous active islanding detection methods, the proposed technique does not require additional control blocks;
2) unlike the majority of passive methods, the proposed method has negligible NDZ;
3) the method is simple and easy to implement since it relies on utilizing the OVP/UVP method.

The simulation results highlight the effectiveness of the proposed islanding detection technique.

APPENDIX

The performance of the proposed islanding detection method as well as its NDZ depend, to a great extent, on the DG P–V characteristic. The NDZ could be calculated by equating the load and DG active power. An active power mismatch of ΔP will result in a voltage deviation of ΔV, which could be expressed as follows:

$$(P)\left(\frac{V}{V_o}\right)^2 = P_{\text{ref}} = aV_{\text{p.u}} + b \qquad (16)$$

$$(P_o + \Delta P)\left(\frac{V_o(1 + \Delta V)}{V_o}\right)^2 = a\left(\frac{V_o(1 + \Delta V)}{V_o}\right) + b \quad (17)$$

where ΔV equal to 0.1 corresponds to the OVP limit (110% of the nominal voltage) while ΔV equal to -0.12 corresponds to the UVP limit (88% of the nominal voltage). From (17)

$$(P_o + \Delta P) = \frac{a(1 + \Delta V) + b}{(1 + \Delta V)^2}. \qquad (18)$$

Table I shows the calculated NDZ for the different values of a and b presented in this paper using (18). Case 1 in Table I, represents the base case where the DG is operating at a fixed power output without the P–V characteristic. It can be seen from Table I that the choice of the P–V characteristic will have an impact on the NDZ. For some cases, the NDZ would increase (Case 3), while for other cases, it would decrease (Case 2).

For Case 4, loads between 98.1 kW and 99.2 kW will intersect the DG P–V characteristic within the OVP/UVP threshold limits. Loads within this range will intersect the DG curve at points where the slope of the DG curve is higher than the slope of the load curve (similar to point D in Fig. 6). Thus, these points are characterized by being unstable operating points and, thus, an islanding condition could be detected easily. Fig. 16 shows the voltage waveform during an islanding condition with an islanded load of 99 kW. It can be seen that once islanding occurs, the voltage deviates and the system becomes unstable. Thus, equipping a DG with the proposed P–V characteristic would result in negligible NDZ.

REFERENCES

[1] S. Jang and K. Kim, "An islanding detection method for distributed generations using voltage unbalance and total harmonic distortion in current," *IEEE Trans. Power Del.*, vol. 19, no. 2, pp. 745–752, Apr. 2004.

[2] M. Ropp and W. Bower, "Evaluation of islanding detection methods for photovoltaic utility interactive power systems," Int. Energy Agency Implementing Agreement on Photovoltaic Power Systems, Tech. Rep. IEA PVPS T5-09, Mar. 2002.

[3] H. Karimi, A. Yazdani, and R. Iravani, "Negative sequence curent injection for fast islanding detection of a distributed resource unit," *IEEE Trans. Power Electron.*, vol. 23, no. 1, pp. 298–307, Jan. 2008.

[4] Z. Ye, R. Walling, L. Garces, R. Zhou, L. Li, and T. Wang, "Study and development of anti-islanding control for grid-connected inverters," General Elect. Global Research Ctr., NREL/SR-560-36243, May 2004.

[5] G. Hernandez-Gonzalez and R. Iravani, "Current injection for active islanding detection of electronically-interfaced distributed resources," *IEEE Trans. Power Del.*, vol. 21, no. 3, pp. 1698–1705, Jul. 2006.

[6] W. Xu, K. Mauch, and S. Martel, "An assessment of DG islanding detection methods and issues for Canada," CANMET Energy Technology Centre-Varennes, Natural Resources Canada, Rep. no. CETC-Varennes 2004-074 (TR), Jul. 2004.

[7] X. Wang, W. Freitas, W. Xu, and V. Dinavahi, "Impact of DG interface controls on the sandia frequency shift antiislanding method," *IEEE Trans. Energy Convers.*, vol. 22, no. 3, pp. 792–794, Sep. 2007.

[8] C. Schauder and H. Mehta, "Vector analysis and control of advanced ststiac VAR compensators," *Proc. Inst. Elect. Eng.*, vol. 15, no. 3, pp. 299–306, Jul. 1993.

[9] *IEEE Standard for Interconnecting Distributed Resources With Electric Power Systems*, IEEE Std. 1547-2003, Jul. 2003.

[10] *Static inverter and charge controllers for use in photovoltaic systems*, UL 1741, Underwriters Laboratories, Inc., 2001, Std. UL.

[11] Z. Ye, A. Kolwalkar, Y. Zhang, P. Du, and R. Walling, "Evaluation of anti-islanding schemes based on nondetection zone concept," *IEEE Trans. Power Electron.*, vol. 19, no. 5, pp. 1171–1176, Sep. 2004.

[12] H. H. Zeineldin, E. F. EI-Saadany, and M. M. A. Salama, "Impact of DG interface control on islanding detection and nondetection zones," *IEEE Trans. Power Del.*, vol. 21, no. 3, pp. 1515–1523, Jul. 2006.

[13] *IEEE Recommended Practice for Monitoring Electric Power Quality*, IEEE Std. 1159–1995, 1995.

[14] D. Koval, W. Xu, and J. Salmon, "Power quality characteristics of rural electric secondary power systems," *IEEE Trans. Ind. Appl.*, vol. 35, no. 2, pp. 332–338, Mar. 1999.

H. H. Zeineldin (M'08) received the B.Sc. and M.Sc. degrees in electrical engineering from Cairo University, Cairo, Egypt, in 1999 and 2002, respectively, and the Ph.D. degree. in electrical and computer engineering from the University of Waterloo, Waterloo, ON, Canada, in 2006.

Dr. Zeineldin was with Smith and Andersen Electrical Engineering, Inc., where he was involved with projects involving distribution system design, protection, and distributed generation. Recently, he joined the Masdar Institute of Science and Technology, Abu Dhabi, United Arab Emirates, and is currently a Visiting Professor at the Massachusetts Institute of Technology (MIT), Cambridge. His current interests include power system protection, distributed generation, and deregulation.

James L. Kirtley, Jr. (F'91) received the Ph.D. degree in electrical engineering from the Massachusetts Institute of Technology (MIT), Cambridge, in 1971.

He has been a member of the faculty of the Department of Electrical Engineering and Computer Science at MIT since 1971, where he is currently Professor of Electrical Engineering. He was also an Electrical Engineer with the Large Steam Turbine Generator at General Electric, General Manager and Chief Scientist with SatCon Technology Corporation, and was Gastdozent at the Swiss Federal Institute of Technology. He is a specialist in electric machinery and electric power systems.

Dr. Kirtley was Editor-in-Chief of the IEEE TRANSACTIONS ON ENERGY CONVERSION from 1998 to 2006 and continues to serve as Editor for that journal and as a member of the Editorial Board of the journal *Electric Power Components and Systems*. He is a member of the U.S. National Academy of Engineering. He was awarded the Nikola Tesla prize in 2002 and the IEEE Third Millennium medal. He is a Registered Professional Engineer in Massachusetts.